Catal Lett (2012) 142:1225–1233
DOI 10.1007/s10562-012-0891-4

One-Step Synthesis of Acetals from Phenol/Alcohols Mixtures Using a Pd/Aluminoborate Catalyst

Yejun Guan · Damin Zhang · Yimeng Wang

Received: 7 June 2012 / Accepted: 9 August 2012 / Published online: 21 August 2012

Abstract A one-step synthesis of cyclohexanone acetals from phenol/alcohol mixtures has been explored using bifunctional aluminum borates supported Pd catalysts. Three aluminum borates have been prepared via either a high temperature calcination ($9Al_2O_3{\cdot}2B_2O_3$) or a self-pressured thermal synthesis (PKU-1 and ABO-X) using various aluminum precursors and boric acid. Well dispersed Pd nanoparticles loaded on these materials show excellent phenol hydrogenation activity in both water and ethanol. The reactivity follows the trend of Pd/ABO-X > $Pd/9Al_2O_3{\cdot}2B_2O_3$ > Pd/PKU-1, which is similar to the sequence of BO_4/BO_3 ratio presented in the aluminoborates as shown by NMR spectra. When ethanol is used as a solvent, 13.5 % yield of cyclohexanone diethyl acetal has been obtained under the conditions investigated on Pd/ABO-X, which is attributed to its high activity in both hydrogenation and acetalization for the one-step synthesis of cyclohexanone acetals.

Keywords Phenol hydrogenation · Palladium · Aluminum borate · Acetalization · Cyclohexanone

1 Introduction

Acetals are an important class of compounds that have found their direct applications in diverse areas in the chemical industry such as perfumes, flavours, pharmaceuticals, solvents, and polymer chemistry [1]. Traditionally, acetalization of aldehydes and ketones is performed using trimethyl orthophosphate in the presence of acid catalysts such as HCl, H_2SO_4, *p*-toluene sulphonic acid and ferric chloride [2]. Cyclohexanone is one of the mostly used ketones and its acetalization has been widely investigated [3, 4], preferably on heterogeneous catalysts [5, 6]. Cyclohexanone itself is industrially produced by partial oxidation of hexane or phenol hydrogenation [7]. It would be beneficial to synthesize cyclohexanone acetal as a one-step synthesis. In this case, the process may start from phenol instead of cyclohexanone. The operation of highly flammable and toxic cyclohexanone is then avoided. To this end, the desired catalyst should be able to hydrogenate phenol first and subsequently catalyze the acetalization reaction. To our knowledge, such a process has not been reported before. Clearly there are several challenges. First, the catalyst should be highly active and selective for phenol hydrogenation to cyclohexanone, otherwise the acetalization will not take place. In fact, supported Pd catalysts are promising for low temperature liquid phase selective hydrogenation of phenol [8–13]. Liu et al. [9] reported a dual supported Pd–Lewis acid catalyst, on which the $AlCl_3$ acts as a Lewis acid and strongly coordinates with cyclohexanone. This suppresses the hydrogenation of cyclohexanone. Some supports, e.g., C_3N_4, MIL-101 and hybrid TiO_2/carbon, are also found to hydrogenate phenol, with 99.9 % selectivity to cyclohexanone at high conversion [10–13]. Second, the catalyst should be acidic enough to catalyze the subsequent acetalization. In this regard, some solid acids like zeolites, Al or Zr incorporated mesoporous materials would be possible candidates [5]. However, palladium supported on these materials seems to show very low activity in hydrogenation under mild conditions

Y. Guan (✉) · D. Zhang · Y. Wang (✉)
Shanghai Key Laboratory of Green Chemistry and Chemical Processes, East China Normal University, North Zhongshan Road 3663, Shanghai 200062, China
e-mail: yjguan@chem.ecnu.edu.cn

Y. Wang
e-mail: ymwang@chem.ecnu.edu.cn

[9, 14]. The incorporation of boron oxide to Al_2O_3 leads to an alumina–boria catalyst with an increase in the acid character which owes to its Bronsted acid sites [15, 16]. In another study, a new zeolitic aluminoborates containing B and Al centers that serve as Lewis acid sites have been also reported [17, 18]. These materials can catalyze alkene isomerization [19], alcohol dehydration [20, 21], and vapor phase Beckmann rearrangement of cyclohexanone oxime [22]. Moreover, doping boron onto alumina surface has been found to be an effective way to increase the hydrogenation activity of supported CoMo or Pt catalysts in oil refinery [23, 24]. Inspired by these studies, we use aluminoborate as a support of palladium to carry out the one-step synthesis of cyclohexanone acetal in this study.

This bifunctional catalyst efficiently converted phenol into cyclohexanone diethyl acetal with ethanol used as a solvent. In contrast, a conventional Al_2O_3 or HZSM-5 supported Pd did not catalyze this reaction. Reaction and characterization results suggest that the crystallized phase and surface structure, most likely the boria groups of aluminum borate play a vital role in determining the one-step synthesis activity.

2 Experimental

2.1 Preparation of Aluminum Borate Supports

a. $9Al_2O_3{\cdot}2B_2O_3$: A conventional calcination synthesis procedure was employed [15, 16]. Typically, 2.4 g of $AlCl_3{\cdot}6H_2O$ and 12.2 g of boric acid were mixed and ground thoroughly. The resulting mixture was heated to 1,200 °C at 10 °C/min and held in static air for 8 h.
b. PKU-1: PKU-1 is a new material synthesized by Ju et al. [17, 18]. In a typical synthesis, 0.76 g of $Al(NO_3){\cdot}9H_2O$ and 12.2 g of boric acid were mixed thoroughly. The resulting mixture was transferred into a Teflon-lined autoclave (50 mL), sealed tightly, and heated in an oven at 240 °C for 4 days. After cooling the autoclave to room temperature, the mixture was dispersed in large amount of water (70 °C) with severe stirring. The hot mixture was subsequently filtered to remove the soluble boric acid, after which the PKU-1 sample was recovered and dried.
c. ABO-X. The synthesis procedure is similar to the one employed for PKU-1. $AlCl_3{\cdot}6H_2O$ was used as aluminum precursor. An unidentified structure was found for the resulting material, which is denoted as ABO-X in this study.

2.2 Preparation of the Supported Pd Catalysts

The supported Pd catalysts were prepared by a deposition-reduction method. Typically, 2.4 mL of H_2PdCl_4 solution (Pd: 18.4 mg/mL) was diluted into 10 mL. It should be noted that the H_2PdCl_4 solution is very acidic, which may partially dissolve the alumina based supports [25]. Therefore, prior to deposition, the pH value of the H_2PdCl_4 solution was adjusted to 6 by dropwise adding 1 M NaOH solution. 0.95 g of support was added into the resulting solution and thoroughly stirred. The final pH value of the mixture was further adjusted to 9 by adding more NaOH solution (1 M). Afterwards, $NaBH_4$ solution was added to the solution in order to reduce the $Pd(OH)_2$ colloid while cooling using ice bath [26]. The solid was filtered and dried at 70 °C under vacuum overnight.

2.3 Characterization

Nitrogen adsorption–desorption isotherms at 77 K were obtained using a BELSORP-max instrument. Prior to measurement, the samples were outgassed at 150 °C under vacuum for 6 h. Specific surface areas were calculated according to the BET-method using five relative pressure points in the interval of 0.05–0.3. The powder X-ray diffraction (XRD) patterns were collected on a Rigaku Ultima IV X-ray diffractometer using Cu Kα radiation ($\lambda = 1.5405$ Å) operated at 35 kV and 25 mA. Scanning electron microscopy (SEM) was performed on a Hitachi S-4800 microscope. Transmission electron microscopy (TEM) images were taken on a JEOL-JEM-2100 microscope at an accelerating voltage of 200 kV. The average Pd particle size was calculated by $d_{TEM} = (\Sigma n_i d_i^3)/(\Sigma n_i d_i^2)$ by measuring at least 100 particles. The Pd loading was determined by a Thermo Elemental IRIS Intrepid II XSP inductively coupled plasma emission spectrometer (ICP-AES). The desired amount of sample was dissolved in 10 mL of aqua regia. This mixture was heated to remove the extra acid and diluted into a 50 mL volumetric flask. ^{11}B and ^{27}Al solid-state magic angle spinning nuclear magnetic resonance (MAS-NMR) spectra were recorded at 20 °C on a Varian 400 MHz spectrometer working at 104.18 MHz (^{27}Al) and 128.27 MHz (^{11}B), with a rotation frequency of 10 kHz and recycle delay of 4 s. The references of ^{27}Al and ^{11}B were taken from $KAl(SO_4)_2{\cdot}12H_2O$ (−0.21 ppm) and $NaBH_4$ (−8.16 ppm), respectively.

2.4 Catalytic Tests

2.4.1 Hydrogenation of Phenol

A teflon-lined (100 mL) steel batch reactor was used to carry out the liquid phase hydrogenation. Prior to reaction, the catalyst (100 mg) was reduced under a H_2 flow at 200 °C for 30 min in a three-neck glass reactor. After cooling down to room temperature, 10 mL of phenol

solution (0.25 M, either of water or of alcohols) was introduced into the glass reactor. The mixture of catalyst and solution was then transferred into the teflon-lined (100 mL) steel batch reactor. The reactor was purged three times with H_2 and then pressurized with 5 bar H_2. The reaction mixture was heated up to 80 °C and held for 4 h. Once the reactor was cooled down, the products were analyzed on a Shimadzu GC 2014 equipped with a RTX-Wax capillary column (30 m length and 0.25 mm internal diameter).

2.4.2 *Acetalization of Cyclohexanone*

Prior to reaction, 10 mg of each sample was loaded in a 50 mL round-bottom flask and dried at 75 °C under vacuum overnight to remove the physisorbed water. After cooling down to room temperature, 5 mL of solvent (methanol or ethanol) was added and 100 μL of cyclohexanone was introduced. The mixture was placed in an oil-bath and refluxed for 1 h at 80 °C for ethanol and 60 °C for methanol, respectively. Then the liquid was filtered, diluted with ethanol, and analyzed on a Shimadzu GC 2014.

3 Results and Discussion

3.1 XRD, BET, SEM and NMR Characterization of Aluminum Borates

Figure 1 shows the XRD patterns of the synthesized aluminum borate supports. When $AlCl_3$ and H_3BO_3 was mixed and calcined at 1,200 °C, the product was orthorhombic $9Al_2O_3{\cdot}2B_2O_3$ (Fig. 1a). This phase is the only one thermodynamically stable upon calcination above 1,000 °C. The surface area of $9Al_2O_3{\cdot}2B_2O_3$ was 111 m^2/g. Using $Al(NO_3){\cdot}9H_2O$ as the precursor, an aluminum borate known as PKU-1 (Fig. 1b) was obtained by self-pressured thermal treatment (240 °C for 4 days). This material had a surface area of 112 m^2/g. With $AlCl_3{\cdot}6H_2O$ being the aluminum precursor, a new aluminum borate with unidentified structure (ABO-X, Fig. 1c) was synthesized using the same thermal treatment. This material had a surface area of 116 m^2/g. No narrow pore distribution is observed for all samples.

Figure 2 shows the SEM images of these materials. Upon high temperature calcination, a complex morphology was observed for $9Al_2O_3{\cdot}2B_2O_3$ (Fig. 2a). Both irregular aggregated particles and long rods were present. Uniformly distributed rods with 1 μm in length and 100 nm in diameter were found for PKU-1 (Fig. 2b), which is consistent with a previous study reported by Ju et al. [17]. ABO-X displayed the same morphology as PKU-1 regardless of crystalline phases, but with non-uniform

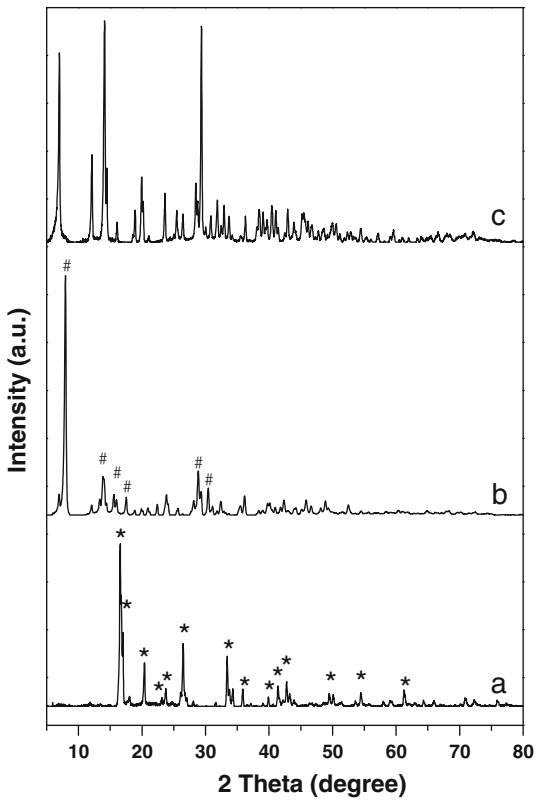

Fig. 1 X-ray diffraction patterns of three aluminum borates:*a* $9Al_2O_3{\cdot}2B_2O_3$ (*),*b* PKU-1 (#), *c* ABO-X

length and width (Fig. 2c). Compared with PKU-1, the diameter of ABO-X was substantially larger. This might be ascribed to the properties of aluminum sources used.

The incorporation of boron to Al_2O_3 leads to an alumina–boria catalyst with an increase in acidity compared to pure Al_2O_3. Acid behavior of the alumina–boria catalyst is reported to be due to bronsted acid sites, which are associated to the boria groups [27–29]. The local environments of B and Al are essential to elucidate the distribution of surface hydroxyl groups. Figure 3a, b display the ^{11}B and ^{27}Al NMR spectra of three aluminum borates, respectively. Distinct differences are clearly observed in these spectra. The crystal structure of the aluminum borate $9Al_2O_3{\cdot}2B_2O_3$ contains four distinct aluminum sites: one tetrahedral, two pentahedral and one octahedral [27]. These resonances can be clearly observed in Fig. 3B-a. Boron is dominated by BO_3 species in $9Al_2O_3{\cdot}2B_2O_3$, as indicated by the characteristic quadrupolar doublet pattern in the range 2–20 ppm. The chemical shift at 0 ppm indicates the coexistence of BO_4 species. BO_4 species are considered to be created by a reversible hydration–dehydration reaction of BO_3 species [19]. Only those BO_3 species situated near the surface are able to transform into BO_4 species, which may be accessible to molecules in catalysis [28, 29]. The NMR spectroscopy of PKU-1 is consistent with previous

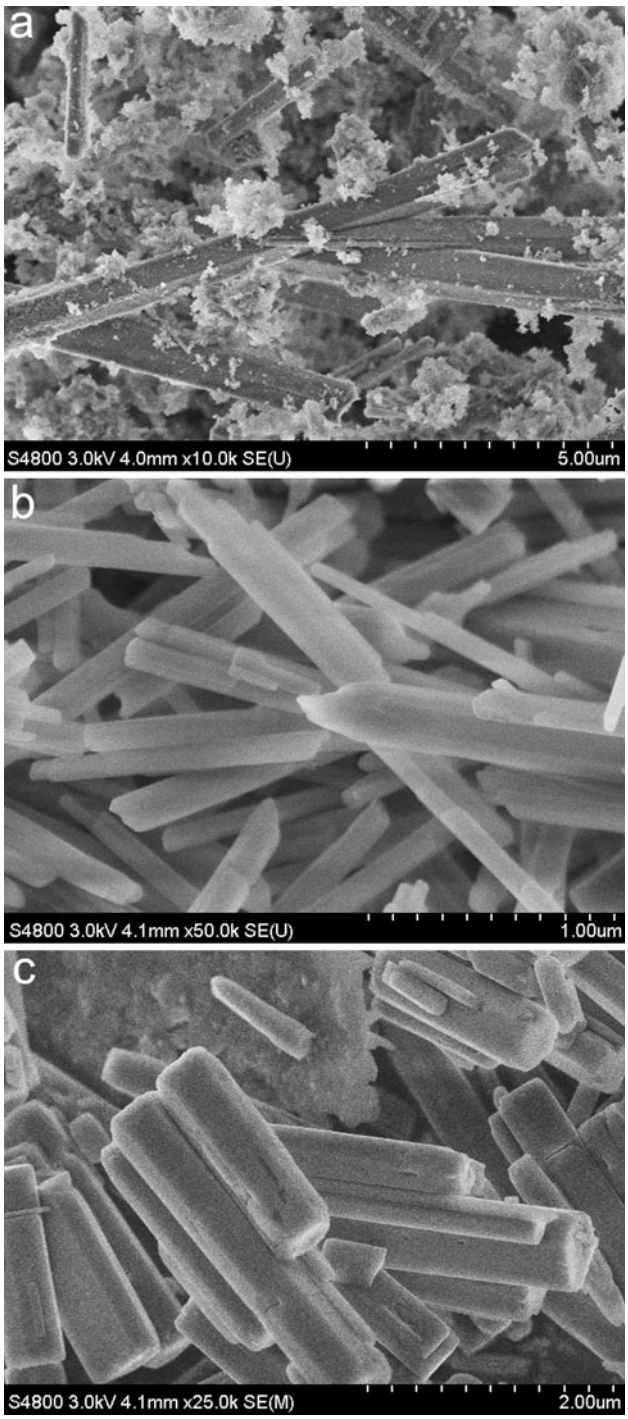

Fig. 2 SEM images of three aluminum borates: **a** $9Al_2O_3{\cdot}2B_2O_3$, **b** PKU-1, **c** ABO-X

reports [17, 18], which is characterized by the quadrupolar doublet pattern. The authors proposed that the Al and B atoms are exclusively in octahedral and triangular coordination, respectively. The structure can be considered as an octahedral framework, which is enveloped by triangular borate groups [i.e., $BO_2(OH)$ and $B_2O_4(OH)$]. These $BO_2(OH)$ and $B_2O_4(OH)$ groups are located within the 18-ring windows and 10-ring rectangular windows, respectively. The ^{11}B NMR of ABO-X was clearly different from both of PKU-1 and $9Al_2O_3{\cdot}2B_2O_3$. A sharp ^{11}B chemical shift was observed centered at 0 ppm. This result means that the boron in ABO-X is mainly present as BO_4 species, with a small fraction of BO_3. The aluminum coordination is similar to that of PKU-1 according to ^{27}Al NMR chemical shift, indicating that the framework also consists of AlO_6 octahedra, which attach to each other by both BO_3 and BO_4 groups. The exact structure still needs to be resolved.

3.2 XRD and TEM Characterization of Pd/Aluminum Borates

Figure 4 displays the XRD patterns of the supported Pd catalysts. The diffraction peak at 40° assigned to the (111) reflection of the Pd nanoparticles was unfortunately overlapped by the strong diffractions of aluminum borates. Accordingly it is not possible to calculate the particle size by using the Scherrer equation. Figure 5 shows the typical TEM images of aluminum borates supported Pd catalysts and the particle size distributions. Well dispersed Pd nanoparticles were found on all catalysts. The average particle sizes of Pd on Al_2O_3 (Fig. 5a), $9Al_2O_3{\cdot}2B_2O_3$ (Fig. 5b), PKU-1 (Fig. 5c), and ABO-X (Fig. 5d) were 8.5, 15, 5, and 6.5 nm, respectively, when $NaBH_4$ was used as a reductant. Clearly boron modified alumina are a group of excellent support materials for the preparation of Pd catalysts. The Pd particle size on $9Al_2O_3{\cdot}2B_2O_3$ was the largest among these catalysts, which may be due to its specific surface property upon high temperature calcination. The effect of reducing reagent was also compared using ABO-X support as an example. Even smaller Pd particles in the range of 1–4 nm (Fig. 5e) were observed when a diluted hydrazine solution was employed as the reducing reagent. It can be concluded that the Pd particle size is dependent on support surface properties and the reducing reagents used.

3.3 Phenol Hydrogenation in Aqueous Solution

The catalysts were tested for the hydrogenation of phenol in aqueous media under mild conditions, i.e. 5 bar of hydrogen and 80 °C for 4 h. Entries 1–4 in Table 1 show the activities of Pd samples obtained using $NaBH_4$ as the reducing reagent. These results show that the catalysts exhibited high selectivity to cyclohexanone under the reaction conditions investigated. $Pd/9Al_2O_3{\cdot}2B_2O_3$ showed 21.2 % of phenol conversion and cyclohexanone selectivity of 81.6 % (Table 1, Entry 1). The phenol conversion on Pd/PKU-1 was higher than that found on $Pd/9Al_2O_3{\cdot}2B_2O_3$, with phenol conversion of 48.5 % and cyclohexanone selectivity of 93.3 % (Table 1, Entry 2). Pd/ABO-X

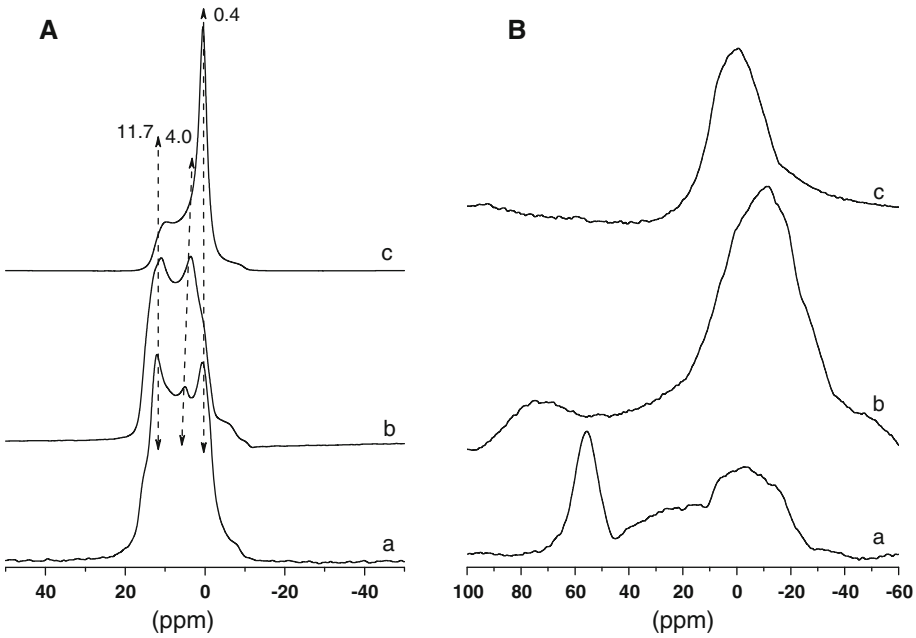

Fig. 3 ^{11}B (**A**) and ^{27}Al NMR (**B**) spectra of three aluminum borates: *a* $9Al_2O_3{\cdot}2B_2O_3$, *b* PKU-1, *c* ABO-X

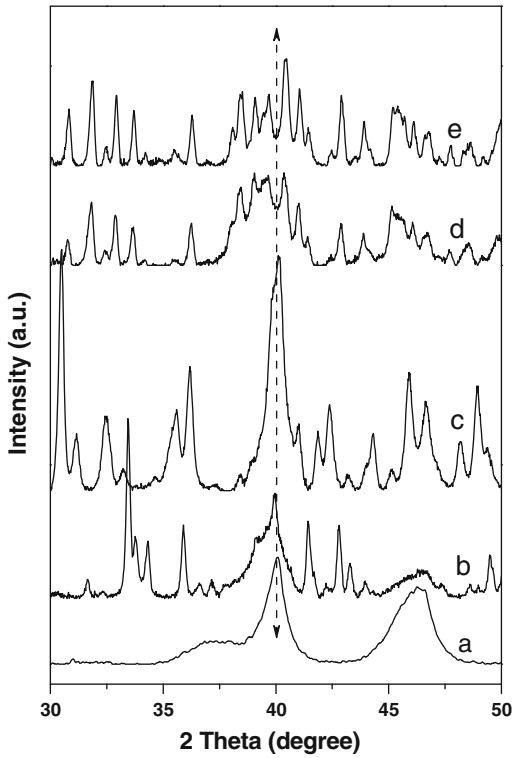

Fig. 4 X-ray diffraction spectra of γ-Al_2O_3 and aluminum borates supported Pd catalysts: *a* Pd/γ-Al_2O_3 ($NaBH_4$), *b* Pd/$9Al_2O_3{\cdot}2B_2O_3$ ($NaBH_4$), *c* Pd/PKU-1 ($NaBH_4$), *d* Pd/ABO-X ($NaBH_4$), *e* Pd/ABO-X (N_2H_4)

showed the best catalytic property among these catalysts, with phenol conversion of 99 % and cyclohexanone selectivity of 99 % (Table 1, Entry 3). This reactivity was comparable to that of Pd/Al_2O_3 (Table 1, Entry 6), but with slightly higher selectivity to cyclohexanone (99 vs. 94.2 %). When the Pd loading was lowered further to 0.88 wt%, this led to a slight decrease of phenol conversion to 94 % (Table 1, Entry 4). In this case, the selectivity to cyclohexanone was as high as 99.6 %. Clearly, ABO-X showed a superior performance as a support of palladium catalysts. Chen et al. [23] proposed that the interaction of boron with Pt metal affected the electronic structure of the metal and the activity for hydrogenation. Another report speculated that the acidic property of B-OH benefited to the interaction between Co–Mo–O groups and support, thus leading to a higher HDS activity [24]. The boria located in the framework as in the case of PKU-1 and $9Al_2O_3{\cdot}2B_2O_3$ does not likely contribute to the hydrogenation activity of Pd. When the diluted hydrazine solution was used as the reducing reagent, much smaller particles with average size of 3 nm were obtained on ABO-X. This catalyst showed comparable activity (Table 1, Entry 5) to that prepared using $NaBH_4$ as the reducing reagent.

3.4 Phenol Hydrogenation and Acetalization Coupling

Given the excellent hydrogenation activity of these aluminum borates supported Pd catalysts in aqueous solution of phenol, we tested their activity for the production of cyclohexanone acetal in a one-step process by combining the phenol hydrogenation and acetalization in an alcohol solution. The results are shown in Table 2. Pd/PKU-1 catalyst did not produce any acetal (Table 2, Entry 1). Under the identical conditions, the other two Pd catalysts were both active for acetal production. Taking Pd/ABO-X as an example, the obtained products contained 50 % of

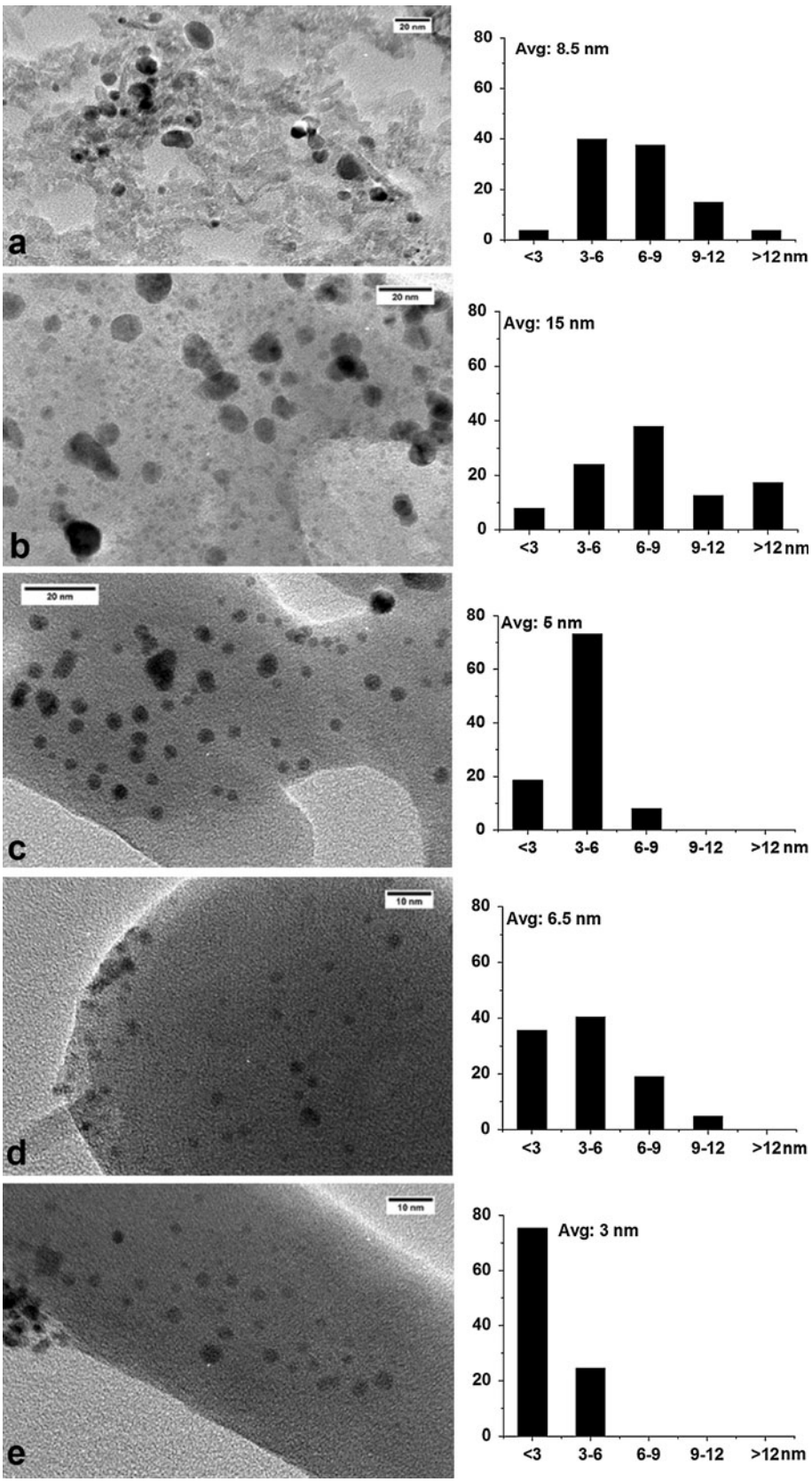

Fig. 5 TEM images and particle distribution of γ-Al_2O_3 and aluminum borates supported Pd catalysts: **a** Pd/γ-Al_2O_3 ($NaBH_4$), **b** Pd/$9Al_2O_3{\cdot}2B_2O_3$ ($NaBH_4$), **c** Pd/PKU-1 ($NaBH_4$), **d** Pd/ABO-X ($NaBH_4$), **e** Pd/ABO-X (N_2H_4)

Table 1 Loading, particle size, and aqueous phase phenol hydrogenation activities of various palladium catalysts

Reaction conditions 10 mL of 0.25 M phenol aqueous solution, 100 mg of catalyst, $T = 80$ °C, $P_{H2} = 0.5$ MPa, $t = 4$ h

[a] Reduced by N_2H_4

Entry	Catalyst	Loading (wt%)	d_{Pd} (nm) TEM	Conv. (%)	Sel. (%)	
					C=O	C–OH
1	$Pd/9Al_2O_3{\cdot}2B_2O_3$	4.6	15	21.2	81.6	18.4
2	Pd/PKU-1	4.7	5.0	48.5	93.3	6.7
3	Pd/ABO-X	5.1	6.5	99.0	99.0	1.0
4	Pd/ABO-X	0.88	n.d.	94.0	99.6	0.4
5	Pd/ABO-X[a]	5.3	3.0	99.4	98.6	1.4
6	Pd/Al_2O_3	5.7	8.5	99.9	94.2	5.8

Table 2 Results of phenol hydrogenation in alcohols on various Pd-based catalysts

Reaction conditions 10 mL of 0.25 M phenol/ethanol (methanol) solution, 100 mg of catalyst, $T = 80$ °C, $P_{H2} = 0.5$ MPa, $t = 4$ h

[a] 100 mg of Pd/Al_2O_3 catalyst and 100 mg of HZSM-5

Entry	Catalyst	Solvent	Conv. (%)	Sel. (%)		
				Acetal	C=O	C–OH
1	Pd/PKU-1	Ethanol	9.1	0.0	92.0	8.0
2	$Pd/9Al_2O_3{\cdot}2B_2O_3$	Ethanol	12.3	19.0	69.0	12.0
3	Pd/ABO-X	Ethanol	45.0	30.0	50.0	20.0
4	Pd/ABO-X (N_2H_4)	Ethanol	30.0	10.0	70.0	20.0
5	Pd/Al_2O_3	Ethanol	62.9	1.1	94.0	4.9
6	Pd/ABO-X	Methanol	4.0	19.5	48.0	32.5
7	Pd/Al_2O_3 + HZSM-5[a]	Ethanol	49.7	27.3	65.7	7.0

cyclohexanone, 20 % of cyclohexanol, and 30 % of cyclohexanone diethyl acetal, with an acetal yield of 13.5 % (Table 2, Entry 3). The yield of acetal for $Pd/9Al_2O_3{\cdot}2B_2O_3$ catalyst was 2.3 % (Table 2, Entry 2). The activity for cyclohexanone dimethyl acetal with methanol as solvent was also investigated using Pd/ABO-X as an example. 19.5 % selectivity to acetal was found but with low phenol conversion (Table 2, Entry 6). It should be noted that Pd/Al_2O_3 only gave trace amount of acetal under the identical reaction conditions (Table 2, Entry 5). The introduction of HZSM-5 (Table 2, Entry 7) to Pd/Al_2O_3 remarkably increased the acetal yield. Apparently, presence of acidic sites is favorable to acetalization. We consider that both the hydrogenation ability of Pd and acidity of support are essential for the production of acetal, as depicted in Scheme 1. Indeed Pd/HZSM-5 barely gave any acetal products in phenol hydrogenation due to its very low hydrogenation activity (not shown), meaning that the interaction between Pd and the acidic site is also relevant. It seems that the metal/support interface may be involved or some specific structures are required for this process. We have investigated the reusability and leaching of Pd catalyst. However, a severe activity loss was found for Pd/ABO-X, for both hydrogenation and acetalization. No leaching of Pd was observed in the hot solution, meaning that the surface property of Pd/ABO-X changed during the hydrogenation process.

Another finding should be noted is that the phenol conversion decreased for all catalysts when ethanol was used as a solvent compared to that observed in water. As an example, the phenol conversion on Pd/ABO-X decreased

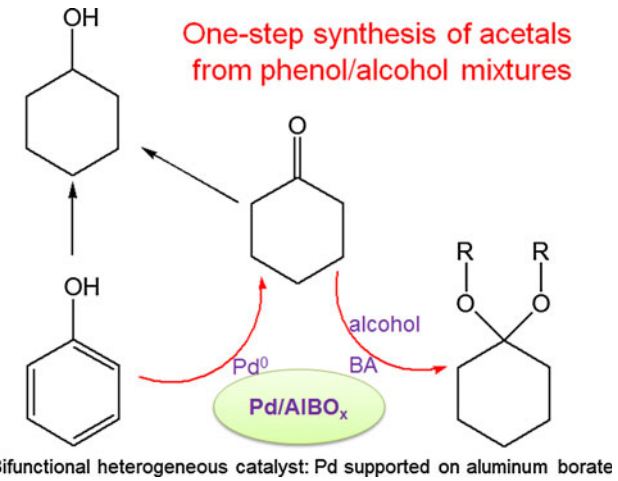

Scheme 1 A schematic illustration of a Pd/aluminum borate catalyst and its bifunctional role in cyclohexanone acetals production from phenol in alcohol

substantially from 99 % (Table 1, Entry 3) to 45 % (Table 2, Entry 3). On the other hand, the selectivity to cyclohexanol increased from 1 % (Table 1, Entry 3) to 20 % (Table 2, Entry 3). This effect is even more pronounced when methanol was used, in which case 4 % of phenol conversion (Table 3, Entry 6) was observed under identical conditions as for Pd/ABO-X. The hydrogenation activity of Pd on ABO-X decreased 10 times when the solvent changed from ethanol to methanol. It should be stressed that Pd/ABO-X was the most active catalyst for phenol hydrogenation in ethanol, whereas Pd/PKU-1 was the least active one. This result indicates that the boron

Table 3 Cyclohexanone acetalization activities on aluminoborates

Sample	Conv. (%)[a]	
	Methanol[b]	Ethanol[c]
PKU-1	0	1.3
$9Al_2O_3{\cdot}2B_2O_3$	2.9	27.2
ABO-X	35.5	17.5
Al_2O_3	0	0
HZSM-5	87.4	55.4

Reaction conditions 10 mg of catalyst, 100 μL of cyclohexanone in 5 mL of alcohol, $t = 1$ h

[a] The conversion was based on cyclohexanone

[b] $T = 60$ °C

[c] $T = 80$ °C

species are likely involved in the phenol adsorption and hydrogenation process. Velu et al. [30] also reported a three-fold drop in phenol conversion using ethanol as a solvent while no product selectivity change was observed. The authors claimed that the drop in phenol conversion could be due to a competitive adsorption of reactants (phenol and/or H_2) and solvents (ethanol) molecules on the same active site [30]. Indeed, the solvent effect is commonly observed in liquid phase hydrogenation, which is usually interpreted by the competitive adsorption of substrates and solvent or solvent dependent hydrogen solubility [31, 32].

3.5 Acetalization of Cyclohexanone with Various Alcohols

To further determine the catalytic role of aluminoborates in acetalization, we have conducted the acetalization of cyclohexanone on these materials, in comparison to that on Al_2O_3 and HZSM-5. The results in various alcohols are listed in Table 3. Alumina showed no activity under the reaction conditions regardless of the type of the alcohols used. In contrast, HZSM-5 showed the highest cyclohexanone conversion, with 87.4 and 55.4 % in methanol and ethanol, respectively. This result emphasizes the importance of bronsted acidity in acetalization. Among aluminum borates, PKU-1 turned out to be the least active one, with 1.3 % cyclohexanone conversion in ethanol and even no conversion in methanol. On $9Al_2O_3{\cdot}2B_2O_3$, the conversion of cyclohexanone was 2.9 and 27.2 % in methanol and ethanol, respectively. Under the identical conditions, the conversion of cyclohexanone on ABO-X was 35.5 and 17.5 % in methanol and ethanol, respectively. The activity of acetalization is in good agreement with that observed in one-step phenol hydrogenation conditions. Properties of the catalyst, such as the number of acid sites, acid strength and pore size have been brought forward previously to explain the acetalization activity [2–4]. Generally speaking, the hydroxyl groups in aluminum borates are associated to boria species, namely BO_3 and BO_4 [19, 28]. Their concentration is more likely ascribed to the number of tetrahedrally coordinated BO_4 sites [15, 19, 29]. ABO-X tentatively presents the most amounts of BO_4 sites among three aluminum borates based on the ^{11}B NMR results. However, we could not determine the exact concentration of surface hydroxyl groups due to their low thermal stability [17]. According to in situ FTIR results, the amount of hydroxyl group decreased fast upon calcination and eventually disappears at 400 °C. No clear trend was found for the activities of $9Al_2O_3{\cdot}2B_2O_3$ and ABO-X in acetalization, as ABO-X was more active than $9Al_2O_3{\cdot}2B_2O_3$ in methanol and vice versa in ethanol. In this study, trace amounts of water in the solvent might adsorb on the surface bronsted acid although all aluminum borates were dried at 75 °C under vacuum overnight prior to the reaction, and thus affected the activity. Indeed, when some aluminum borates (PKU-1 and PKU-2) were used for acid-catalyzed reactions, the samples needed to be dried thoroughly and the solvent should be degassed prior to reactions [18]. In summary, these results suggest that aluminum borates are indeed active in acetalization and their activities are dependent on the surface properties.

4 Conclusion

Crystallized aluminum borate materials with distinct various structures and morphologies were synthesized by different methods. These materials have different ratios of BO_4/BO_3 species, following the trend of ABO-X > $9Al_2O_3{\cdot}2B_2O_3$ > PKU-1. The presence of BO_4 species contributes to both the acidity of the obtained aluminum borates and the phenol hydrogenation activity of supported Pd nanoparticles. Pd/ABO-X catalyst shows the highest hydrogenation activity for phenol in water and ethanol. Moreover, a one-step synthesis of cyclohexanone diethyl acetal on Pd/ABO-X catalyst is achieved by simple hydrogenation of phenol in an ethanol solution.

References

1. Perez-Mayoral E, Martin-Aranda RM, Lopez-Peinado AJ, Ballesteros P, Zukal A, Cejka J (2009) Top Catal 52:148
2. Thomas B, Prathapan S, Sugunan S (2005) Microporous Mesoporous Mater 80:65
3. Iwamoto M, Tanaka Y, Sawamura N, Namba S (2003) J Am Chem Soc 125:13032
4. Jermy BR, Pandurangan A (2006) J Mol Catal A 256:184
5. Carrillo AI, Serrano E, Luque R, Matinez JG (2010) Chem Commun 46:5163

6. Rajabi F, Balu AM, Torenia F, Luque R (2011) Catal Sci Technol 1:1051
7. Dimian AC, Bildea CS (2008) Phenol hydrogenation to cyclohexanone, in chemical process design: computer-aided case studies. Wiley-VCH Verlag Gmbh & KGaA, Wienheim
8. Makowski P, Cakan RD, Antonietti M, Goettmann F, Titirici MM (2008) Chem Commun 999
9. Liu HZ, Jiang T, Han BX, Liang SG, Zhou YX (2009) Science 326:1250
10. Wang Y, Yao J, Li HR, Su DS, Antonietti M (2011) J Am Chem Soc 133:2362
11. Liu HL, Li YW, Luque R, Jiang HF (2011) Adv Synth Catal 353:3107
12. Matos J, Corma A (2011) Appl Catal A 404:103
13. Perez Y, Fajardo M, Corma A (2011) Catal Commun 12:1071
14. Mori K, Furubayashi K, Okada S, Yamashita H (2012) Chem Commun 48:8886
15. Bautista FM, Campelo JM, Garcia A, Luna D, Marinas JM, Moreno MC, Romero AA, Navio JA, Macias M (1998) J Catal 173:333
16. Abbas-Ghaleb R, Garbowski E, Kaddouri A, Gelin P (2006) Catal Today 117:514
17. Ju J, Lin JH, Li GB, Yang T, Li HM, Liao FH, Loong CK, You LP (2003) Angew Chem Int Ed 42:5607
18. Yang T, Bartoszewicz A, Ju J, Sun JL, Liu Z, Zou XD, Wang YX, Li GB, Liao FH, Martin-Matute B, Lin JH (2011) Angew Chem Int Ed 50:12555
19. Sato S, Kuroki M, Sodesawa T, Nozaki F, Maciel GE (1995) J Mol Catal 104:171
20. Wang WJ, Chen YW (1991) Catal Lett 10:297
21. Xiu TP, Wang JC, Liu Q (2011) Microporous Mesoporous Mater 143:362
22. Forni L, Fornasari G, Tosi C, Trifiro F, Vaccari A, Dumeignil F, Grimblot J (2003) Appl Catal A 248:47
23. Chen YW, Li CP (1992) Catal Lett 13:359
24. Li CP, Chen YW, Yang SJ, Wu JC (1993) Ind Eng Chem Res 32:1573
25. Balint I, Miyazaki A, Aika K (2001) Chem Mater 13:932
26. Toebes ML, van Dillen JA, de Jong KP (2001) J Mol Catal A 173:75
27. Massiot D, Muller D, Hubert Th, Schneider M, Kentgens APM, Cote B, Coutures JP, Gessner W (1995) Solid State Nucl Magn Reson 5:175
28. Dumeignil F, Rigole M, Guelton M, Grimblot J (2005) Chem Mater 17:2361
29. Dumeignil F, Rigole M, Guelton M, Grimblot J (2005) Chem Mater 17:2369
30. Velu S, Kappor MP, Inagaki S, Suzuki K (2003) Appl Catal A 245:317
31. Singh UK, Vannice MA (2001) Appl Catal A 213:1
32. Takagi H, Isoda T, Kusakabe K, Morooka S (1999) Energy Fuel 13:1191